

Cover Page



Universiteit Leiden



The handle <http://hdl.handle.net/1887/21704> holds various files of this Leiden University dissertation

Author: Gupta, Vikas

Title: Multimodality cardiac image analysis for the assessment of coronary artery disease

Issue Date: 2013-09-11

2

A survey of Cardiac MR image processing methods

This chapter was adapted from:

V. Gupta, H. A. Kirişli, E. A. Hendriks, M. van de Giessen, R. J. van der Geest, W. J. Niessen, J. H. C. Reiber, and B. P. F. Lelieveldt. **Cardiac MR perfusion image processing techniques: A Survey**, *Medical Image Analysis*, Volume 16, Issue 4, Pages 767–785, 2012.

Abstract

First-pass cardiac MR perfusion (CMRP) imaging has undergone rapid technical advancements in recent years. Although the efficacy of CMRP imaging in the assessment of coronary artery diseases (CAD) has been proven, its clinical use is still limited. This limitation stems, in part, from manual interaction required to quantitatively analyze the large amount of data. This process is tedious, time-consuming, and prone to operator bias. Furthermore, acquisition and patient related image artifacts reduce the accuracy of quantitative perfusion assessment. With the advent of semi- and fully automatic image processing methods, not only the challenges posed by these artifacts have been overcome to a large extent, but a significant reduction has also been achieved in analysis time and operator bias. Despite an extensive literature on such image processing methods, to date, no survey has been performed to discuss this dynamic field. The purpose of this chapter is to provide an overview of the current state of the field with a categorical study, along with a future perspective on the clinical acceptance of image processing methods in the diagnosis of CAD.

MONITORING blood circulation through the myocardium provides valuable information about the health of myocardial tissue [114, 145], and helps in diagnosing coronary artery disease (CAD) at an early stage. Myocardial perfusion is a strong indicator of the functional integrity of the myocardium. As such, imaging techniques that allow non-invasive monitoring of the coronary circulation play an important role in detecting perfusion defects. SPECT and PET have been used most commonly for myocardial perfusion assessment [65, 89, 96, 103, 193, 211], and first-pass cardiac MR perfusion (CMRP) imaging is rapidly gaining ground. The growth of CMRP imaging can be attributed to its non-ionizing property and versatility in providing insights into the functional, as well as the anatomical aspects of myocardial perfusion. A few studies have also shown that CMRP imaging compares favorably with SPECT and PET [195, 212, 250]. In addition, its higher spatial resolution helps in detecting, for instance, sub-endocardial layer infarcts [16, 211], which are difficult to detect in SPECT and PET images.

In CMRP imaging, the changes within the myocardium are studied by monitoring the first pass of a contrast agent through the heart with Electrocardiogram (ECG)-gated MR images (Figure 2.1). The myocardial perfusion reserve is, generally, estimated by comparing MR images at stress and rest; stress images are acquired by using vasodilators such as adenosine or dipyridamole [118, 185, 259]. The uptake of contrast agent by myocardial tissue induces signal intensity variation due to shortening of the T1 relaxation time, which leads to a brighter signal when a T1-weighted imaging sequence is employed. An important manifestation of this signal intensity variation is the hypointensity in certain regions due to lower regional blood supply that might be an indicator of myocardial ischemia [202]. The interpretation of CMRP images is therefore essential in the early diagnosis of CAD. A CMRP scan is usually followed by a quantitative analysis of the myocardial perfusion from the acquired images in order to identify and locate the abnormal or vulnerable myocardial region(s). Although the manual interaction in this analysis allows reliable detection of a CAD in a clinical setting, it is often time-consuming, tedious, and prone to inter- or intra-observer measurement variability. A further complication in the quantitative analysis is introduced by the acquisition and patient related image artifacts. To reduce the manual interaction, operator bias, and the effect of artifacts (e.g., motion artifacts), several semi- and fully- automated image processing methods have been developed. These methods have been shown to overcome the problems associated with image artifacts and to significantly reduce both the measurement variability and the analysis time.

Rapid developments in the field of CMRP image processing have resulted in an extensive literature over the last two decades. The objective of this paper is to provide a survey of such a literature. Our methodology involved the screening of all the publications related to CMRP image processing in last 20 years (until November 2010) with following keywords: *mr perfusion*, *cardiac mr perfusion* and *first-pass myocardial perfusion*. All major international journals and conference proceedings were screened for the papers that were within the scope of this survey. This ensures a comprehensive coverage of all the peer-reviewed literature that is available online. However, in those cases wherein more than one article was published by the same author(s) on the same method (e.g., a conference paper extended into a journal paper), we selected the latest of the published papers, preferably a journal publication.

The organization of this chapter is as follows. In Section 2.1, we briefly introduce

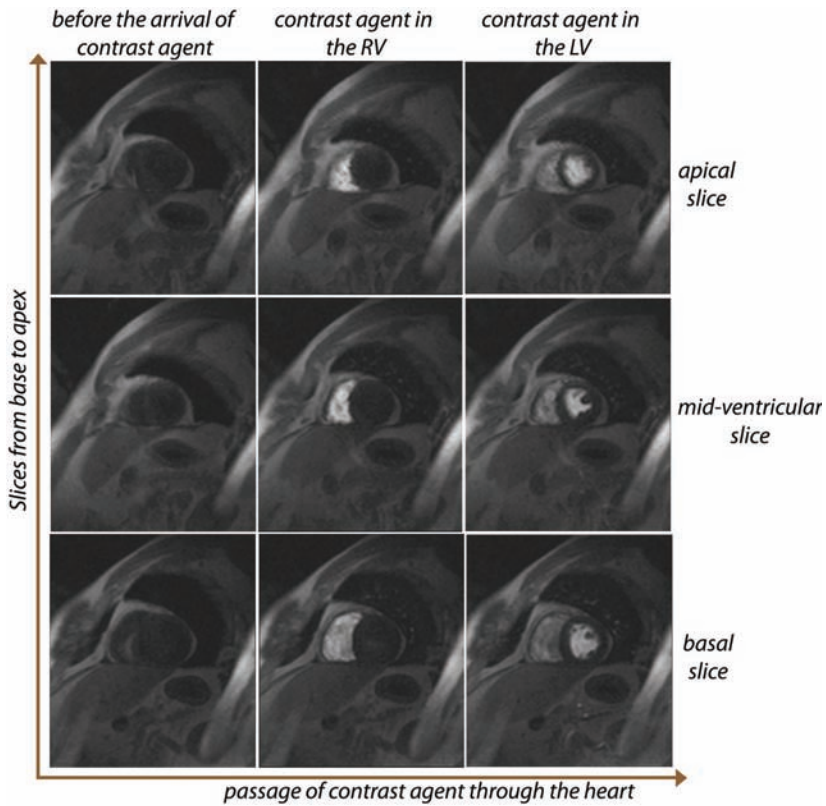


Figure 2.1: An example of first pass cardiac MR perfusion (CMRP) images: the columns show three time-frames from a CMRP sequence representing the passage of a contrast agent through the right ventricle (RV) and the left ventricle (LV). The images acquired before the contrast uptake by cardiac tissue form the leftmost column. Each row shows a different slice.

CMRP image acquisition components, perfusion quantification, and the major artifacts related to CMRP images. Sections 2.2, 2.3, 2.4, and 2.5 form the core of this chapter wherein we categorize the existing literature, and discuss the main ideas of surveyed methods within their respective categories. In Section 2.6, we provide a summary of the current and future trends in CMRP image processing, and conclude with the future perspectives on their clinical acceptance.

2.1 Background

2.1.1 Cardiac MR perfusion (CMRP) image acquisition

A typical acquisition procedure for CMRP images involves a combination of three major components: a contrast agent, a pre-pulse scheme, and an imaging sequence. The use of an external contrast enhancing substance, such as gadolinium, was first introduced in the late 1980s [39, 153]. This was soon followed by the development of a technique by

Atkinson et al.[13] in 1990, which allowed the dynamic evaluation of perfusion images using first-pass of the contrast agent. Since then, MR has been employed extensively to study myocardial perfusion both in laboratory animals and in humans [6, 20, 21, 40, 58, 71, 79, 104, 127, 134, 144, 155, 175, 178, 202, 242, 245, 272].

Contrast in CMRP images can be induced either with the injection of exogenous (originating from outside the body) contrast agents or endogenously using a physiological phenomenon. One of the most widely used *exogenous* contrast agents is gadolinium which, due to its extreme toxicity in free form, is always chelated. Contrast agents, such as Gd-DTPA (Gadolinium-Diethylene Triamine Pentaacetic Acid), alter the local magnetic field, and thereby enhance the relaxation rate of water protons in close proximity to the contrast agent. This results in an enhanced signal from the tissues that are perfused [192, 253, 255]. Nevertheless, an analysis based on the assumption that signal intensity enhancement within the myocardium depends on pure myocardial perfusion can result in an inaccurate diagnosis, as about half of the contrast agent leaks into the interstitial space during the first pass [240, 241]. It must therefore be taken into account during quantitative image analysis that the myocardial signal intensity does not depend only on tissue blood volume and perfusion, but also on diffusion. In case a gadolinium based contrast agent is employed, patients with chronic renal insufficiency should be identified, and prophylactic measures should be taken to reduce the risk of nephrotoxicity [28, 196, 238]. *Endogenous* contrast based approaches use blood flow and oxygenated related endogenous contrast instead of the contrast induced by an exogenous substance. Most prominent among them use spin labeling [75], blood oxygen level dependent (BOLD) contrast [76, 128] and magnetization transfer contrast [261, 262].

Table 2.1 summarizes widely used pre-pulse schemes and imaging sequence protocols along with their advantages and disadvantages. Pre-pulse or magnetization preparation schemes are used to modify T1 contrast or suppress signal from specific tissues or regions [179]. As shown in the table, inversion recovery and saturation recovery are the two main types of pre-pulse schemes. In the earlier days of CMRP imaging (1990-1995), the inversion recovery pre-pulse was frequently used due to its ability to produce a higher contrast between hypo- and hyper-perfused tissues. However, despite its higher contrast producing abilities, the inversion recovery scheme suffered from longer acquisition times, limited temporal resolution and lesser reliability in case of arrhythmias. With the introduction of saturation recovery in 1995 [242], the disadvantages of inversion recovery were overcome at the expense of reduced signal contrast. Moreover, due to its insensitivity to arrhythmias and shorter acquisition time, it became possible to incorporate multi-slice coverage, thereby improving temporal resolution. Usually, 3-6 slices are acquired with a temporal resolution of 150 milliseconds/slice (varying with number of slices and the heart rate) to enable the detection of large-vessel CAD. Images at each slice location are generally acquired over 40-60 cardiac cycles, which results in the corresponding number of phases for each slice. The z-resolution is limited by the number of slices that can be acquired within one cardiac cycle. The spatial resolution of CMRP images depends on various factors such as spatial coverage, heart rate, field of view, imaging sequence, etc., which are varied to achieve an adequate spatial resolution for the detection of sub-endocardial defects (< 3mm in-plane) and the assessment of their transmural [118]; a typical image therefore has an in-plane spatial resolution of 2–3 mm.

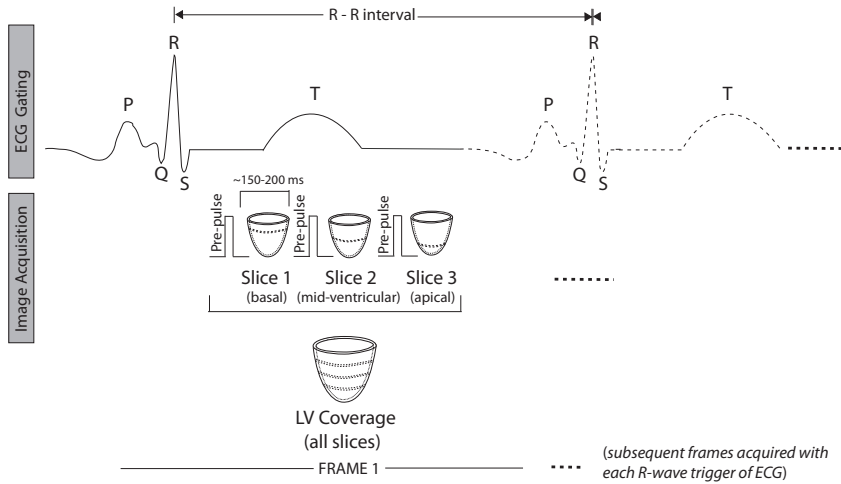


Figure 2.2: Typical CMRP image acquisition process: The cardiac contraction is frozen by synchronizing the image acquisition to the heart cycle using the R-wave on the ECG as a trigger signal for the scanner.

Another important component of CMRP image acquisition is the image sequence protocol as shown in Figure 2.2 and Table 2.1. The most commonly used sequences for CMRP imaging are: spoiled gradient-recalled echo (GRE), balanced Steady state free precession (bSSFP), and Hybrid echo-planar imaging (EPI) [179]. In addition, faster image acquisition and higher spatial resolution can be achieved by using parallel imaging (e.g., with spoiled GRE) as it exploits the spatial distribution of array coil elements in reducing the amount of phase encoding [179] steps (e.g., k-space sampling) required to reconstruct the image. This reconstruction is performed either in the k-space with simultaneous acquisition of spatial harmonics (SMASH) [222], or in image domain using SENSE [183]. Presently, CMRP image acquisition is most commonly performed at 1.5 Tesla, but acquisitions at 3.0 Tesla are becoming increasingly popular as a higher field strength has been shown to improve both, contrast to noise (CNR) and signal to noise ratios (SNR) [49].

Recent technical advancements notwithstanding, the image acquisition components are also associated with specific image artifacts (section 2.1.3). The contribution of these artifact mechanisms is generally influenced by the choice of imaging sequence as well as the other acquisition components, such as pre-pulse scheme and contrast agent. Moreover, with technical developments, such as high field strengths (e.g., 3T), potential of artifacts in the images may also increase significantly.

2.1.2 Perfusion quantification

Perfusion quantification refers to the assessment of myocardial blood flow with quantitative, observer-independent, and reproducible measures, which can provide new insights into the etiology of CADs. These measures rely on the rate at which the contrast agent arrives in myocardial tissue and the signal enhancement induced by this arrival. Typically,

Table 2.1: Advantages and disadvantages of the commonly used image acquisition parameters

Type	Advantages	Disadvantages
Pre-pulse		
<i>Inversion recovery</i>	High signal contrast between hypo- and normally perfused tissues	Less reliable in arrhythmias Long acquisition time Low temporal resolution
<i>Saturation recovery</i>	Shorter acquisition window High temporal resolution Insensitive to arrhythmias	Less signal contrast between hypo- and normally perfused tissues
Imaging sequence		
<i>Spoiled gradient-recalled echo (GRE)</i>	Shorter repetition times	Lower SNR and CNR due to lower flip angles Long acquisition time per image limits maximum heart rate for the acquisition
<i>Balanced steady state free precession (bSSFP)</i>	Highest CNR	Most susceptible to artifacts, especially dark banding artifacts
<i>Hybrid echo planar imaging (EPI)</i>	Higher CNR due to higher flip angles Fast imaging due to shorter acquisition time per image	Low SNR Ghosting effects

the myocardial blood flow is quoted as arterial input rate (mL/min) per gram of tissue, which gives *mL/min per g of tissue* as the unit of myocardial blood flow [110]. Two kinds of approaches exist for perfusion quantification: (a) semi-quantitative analysis, and (b) absolute quantification.

Semi-quantitative analysis

Semi-quantitative analysis of myocardial perfusion has been shown to improve the sensitivity and specificity of CMRP image analysis in detecting significant stenoses [58, 126, 161, 258]. Such an analysis can be performed with the perfusion parameters that are obtained by analyzing the time-intensity curves (TIC). A TIC (Figure 2.3) represents the sampled myocardial intensity in a CMRP image sequence for all the time points within a region of interest (ROI). The initial constant segment of this TIC is called the *baseline*, which represents the time points before the arrival of contrast agent into the ventricles. The most commonly used perfusion parameters are provided in the following list; among these, the *up-slope* and *myocardial perfusion reserve index* have been considered as the most relevant semi-quantitative parameters for the detection of a perfusion abnormality.

- a. *Peak signal intensity (SI_{peak})*: The peak value of the TIC attained during the first pass of the contrast agent, relative to the baseline before contrast enhancement [117].
- b. *Up-slope*: The first derivative of the TIC during the initial ascent of the first pass. The up-slope of the myocardium is usually normalized by the up-slope of LV blood pool to correct for differences of the speed and compactness of the contrast agent bolus [6, 162, 212].

- c. *Time to peak* (T_{peak}): The time from the onset of contrast enhancement (called as the 'foot') to the SI_{peak} .
- d. *Mean transit time* (T_{mean}): The average time required for a contrast agent to pass through the ROI [117].
- e. *Area under the TIC* (A_{TIC}): The area under the TIC from the beginning of its ascent to a user-defined point.
- f. *Myocardial perfusion reserve index* (MPRI): The MPRI is defined as the ratio of hyperemic and basal myocardial blood flow. Generally, MPRI is estimated as the ratio of the normalized up-slopes measured for rest and stress images [7, 112].

A recurring problem with the computation of these parameters is the disruptive changes in the TIC due to noise and the artifacts such as Gibbs ringing [110]. As a result, the distortion of the TIC may also introduce ambiguities in selecting the points for the computation of the *baseline*, the *foot*, and the *up-slope*, which subsequently leads to incorrect estimation of other semi-quantitative parameters (e.g., MPRI). It is therefore important that the user must be aware of these pitfalls during the semi-quantitative analysis of CMRP images.

Absolute perfusion quantification

Absolute quantification is often performed to gain more insights into the coronary physiology as the global reduction in patients with multi-vessel disease makes the semi-quantitative analysis inadequate [14]. Moreover, the absolute quantification was found to be more closely correlated with the gold standard for regional tissue perfusion, *i.e.*, microsphere blood flow, than the semi-quantitative perfusion parameters [50, 51, 111, 159]. Absolute quantification approaches can be either: (a) model-based, or (b) model independent; the model refers to spaces in myocardial tissue structure and their behavior defined by a set of mathematical functions [110, 135]. Whereas model-based approaches are often based on compartmental analysis, model-independent approaches are based on central volume principle [273–275]. For more details on quantification approaches to assess myocardial blood flow, we encourage the reader to refer to the comprehensive review articles by Jerosch-Herold et al.[110], Attili et al.[14], and Christiansen et al.[52].

2.1.3 CMRP image artifacts

CMRP images are often associated with one or more artifacts that can distort the quantitative image analysis results. While some of those artifacts are attributed to the acquisition system, others are related to the patient itself (e.g., motion artifacts). Acquisition related artifacts (e.g., surface coil inhomogeneity, dark rim artifacts) may alter the time intensity curves, and hence, prevent accurate quantitative analysis. Following are the major artifacts associated with CMRP images and the corresponding acquisition based solutions:

2.1.3.1 Surface coil inhomogeneity

Surface coils are used to improve the SNR in MR images. However, as the sensitivity of the coil falls rapidly with distance from the coil, intensity inhomogeneities are introduced in the images. These inhomogeneities can have a significant effect on the quality of

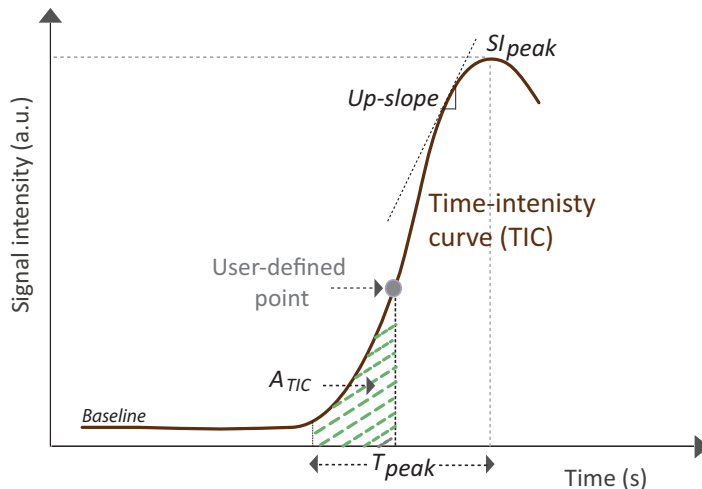


Figure 2.3: A time-intensity curve (TIC) and semi-quantitative perfusion parameters

acquired images [15, 25]. The surface coil induced intensity inhomogeneity can partially be compensated by using two surface coils on either side of the body. A commonly used solution, specific to myocardial perfusion imaging, involves the use of adiabatic (B1-insensitive), RF inversion or saturation pulses, or composite pulses [110]. Post-acquisition, the CMRP images can be corrected for intrinsic spatial signal intensity variations within the myocardium by baseline correction, which involves the normalization of myocardial signal by its pre-contrast value [110]. More details on the intensity inhomogeneity correction methods for MR images can be found in [25, 118]; and [110].

2.1.3.2 Dark rim artifacts

Dark rim artifacts (DRA) appear as a dark sub-endocardial rim that may be confused with actual hypo-intense regions as a result of reduced blood flow. There have been several studies on the causes of DRA [9, 10, 64, 207, 230], and the following have been agreed upon as the most probable:

- a. *Gibbs ringing* is usually caused by truncation or the non-uniformity of the k-space weighting; the non-uniformity across k-space leads to point spread function (PSF) distortion causing both blurring (loss of spatial resolution) and edge enhancement [64]. The Gibbs's ringing can be partially mitigated at the expense of spatial resolution by windowing or apodization, which involves the k-space filtering with a window function [88, 118].
- b. *Partial Volume effect* arises due to the spill-over of signals from neighboring tissues. It may also give rise to dark rim artifacts at the border of the LV blood pool and the endocardium [64, 118], thus making the segmentation of endocardial wall more difficult. A solution to this problem was suggested and validated by Kostler et al. [131] who added a "spillover" term to their myocardial contrast enhancement

model. The “spillover” term was calculated by applying variable scaling and time-shift to the arterial input function.

- c. *Band effect* occurs at the tissue boundaries when the object moves between the acquisitions of different phase encoding lines [230]. These effects can be mitigated by shim re-adjustment [118] or parallel imaging [88].

2.1.3.3 Motion artifacts

The displacement or deformation of the heart during CMRP image acquisition leads to motion artifacts. These artifacts are introduced mainly due to: (a) cardiac motion during pumping of the blood, and (b) respiratory motion during image acquisition. In general, motion artifacts introduce blurring, ghosting, and mis-registrations [210].

a. *Cardiac motion artifacts*

These artifacts are eliminated by means of ECG gating and by acquiring the images during the filling phase of the cardiac cycle when the heart is relatively stationary. This phase begins at the R wave of the ECG after the relatively heart-rate invariant systolic phase [254]. Nevertheless, there still remains a possibility of the triggering faults that may result in blurring or deformation of the heart image.

b. *Respiratory motion artifacts*

Respiratory motion induced artifacts are the most commonly observed patient related artifacts in CMRP images. Several studies have been conducted to determine the effect of respiration [105, 215] and to quantify the rigid and non-rigid motion of the heart with respiration [147]. McLeish et al.[147] showed that the motion of the heart is predominantly linear with diaphragm in the superior-inferior direction. The extent of this movement, however, varies substantially with respiratory phases (inspiratory or expiratory), diaphragm location, and between patients. Furthermore, as shown by Wang et al.[252], respiratory motion of the heart can be decomposed into uniform and non-uniform constituents; while the former is roughly approximated as global translation, the latter is the difference between motion at the center and edge of the field of view. A more comprehensive discussion on motion in cardiovascular imaging was provided in [215].

Although it is possible to perform CMRP image acquisition on free-breathing patients, breath-hold based acquisition is more popular as it allows for the compensation of respiratory motion artifacts. For a breath-hold based acquisition, the patient is asked to hold his/her breath for 45-50 seconds. In addition, ECG based triggering ensures that the motion of the heart is effectively frozen during the acquisition of images over multiple cardiac cycles. However, a prolonged single breath hold in many patients, especially those with CADs, leads to sudden respiration during the image acquisition, and as a consequence, to displacement and/or deformation of the heart.

The limitations of acquisition based strategies in eliminating motion artifacts necessitated the development of post-processing techniques, which apply corrections in either k-space, such as autofocus [12], motion decoupling [269]) etc., or in image domain (sections 2.2, 2.3, and 2.4). In general, image domain techniques have been shown to

perform significantly better as they have inherently less limitations in correcting complex spatial domain deformations than the k-space based techniques [147]. The detailed discussion on such image domain based techniques is provided in subsequent sections.

Table 2.2: Abbreviations and notations

Name	Description
AAM	Active Appearance Modeling
ASSERT	Adaptive Semi-automatic and Self-evaluated Registration Technique
BEP	Bull's Eye Plot
CC	Cross-Correlation
CMRP	Cardiac Magnetic Resonance Perfusion
CT	Computed Tomography
CTCA	Computed Tomography based Coronary Angiography
DE-MR	Delayed Enhancement MR
EPI	Echo-Planar Imaging
FAME	A Flexible Appearance Modeling Environment
FAMIS	Factor Analysis for Medical Image Segmentation
FFD	Free-form Deformation
GRE	Gradient Recalled Echo
GVF	Gradient Vector Flow
ICA	Independent Component Analysis
LV	Left ventricle
MDL	Minimum Description Length
MI	Mutual Information
MPRI	Myocardial Perfusion Reserve Index
MSD	Mean Squared Differences
NGF	Normalized Gradient Fields
NMI	Normalized Mutual Information
PD	Proton Density
PLSR	Partial Least Squares Regression
PVE	Partial Volume Effect
RV	Right Ventricle
SD	Standard Deviation
SENSE	Sensitivity Encoding for fast MRI
SMASH	Simultaneous Acquisition of Spatial Harmonics
SSD	Sum of Squared Differences
bSSFP	Balanced Steady State Free Precession
STACS	Stochastic Active Contour Scheme
TIC	Time Intensity Curve
VBEP	Volumetric Bull's Eye Plot
WH-MR	Whole Heart MR

2.2 Classification of CMRP image processing methods

Interpretation of CMRP images requires image processing methods that help in effectively extracting and quantifying the diagnostic information. More specifically, these methods should be able to: (a) ensure the spatial correspondence between the images in the CMRP sequence, (b) address the problems associated with the presence of anatomical structures (e.g., lungs, diaphragm, trabeculae, etc.) and low contrast around the myocardium, and (c) distinguish the perfusion defect induced intensity variations from those due to noise and artifacts. To address all or most of these requirements, several methods have been proposed. The majority of these methods involve either a registration or a segmentation component, but a few methods also employ both in succession or in a feedback loop. Registration is required to ensure the spatial correspondence (to eliminate motion artifacts) and segmentation helps in the semi- or fully automatic identification and delineation of the region of interest for diagnostic assessment.

Visualization of the extracted information after registration and segmentation is another task that has gained popularity in recent years. The importance of visualization

techniques has been enhanced by the requirement of multi-modality information fusion to present multiple parameters (e.g., perfusion parameters from CMRP images and structural information from Computed Tomography based Coronary Angiography (CTCA) images) in an integrated yet intuitive display.

To present all the methods in a systematic fashion, we have classified CMRP image processing methods into two broad categories on the basis of the major components *i.e.*, registration and segmentation. In addition, a separate category has been dedicated to the discussion of multi-modality information fusion and visualization approaches. All these categories are followed by a summary of the common traits observed in the reviewed approaches along with their advantages and disadvantages. It must be noted that in the event of one method consisting of both a registration and a segmentation technique, it is included in the category closer to its major component.

2.3 Methods based on registration

Registration involves aligning the different images of the same object into strict spatial congruence by applying a suitable transformation. Figure 2.4 shows a typical registration pipeline. Methods to geometrically align CMRP images use either: (a) rigid transformation based registration, or (b) non-rigid/elastic transformation based registration. This spatial alignment is performed with a *target* image that has to be transformed and a fixed *reference* image by using an optimizer. The optimizer (e.g., least squares, gradient descent, etc.) controls the iterative registration process to achieve a desired spatial correspondence between the *target* and the *reference* images. If the transformation results in points that do not coincide with the regular grid, an interpolation scheme is required to determine the intensity value of those points at non-grid positions. Among the most common interpolation strategies are: bilinear, bicubic, splines, and nearest neighbor interpolation.

Registration schemes can often be computationally expensive and prone to the influence of undesired regions in the target and reference images. Limiting the processing to a region of interest (ROI) helps in eliminating the interference from surrounding structures thereby increasing the efficiency of the registration. The accuracy of spatial correspondence or registration between the transformed *target* and the *reference* images is provided by the similarity metric, which is a major constituent of a typical registration pipeline (Figure 2.4). In some cases, a similarity function controls both the evaluation of the quality of registration and the optimization procedure.

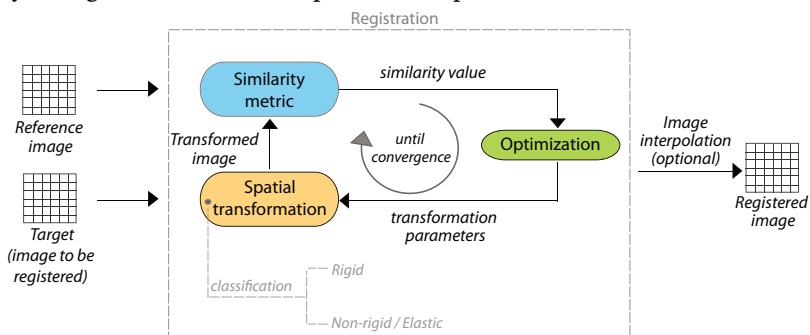


Figure 2.4: A typical registration scheme depicting its different steps and components

Table 2.3: Registration based methods

Authors	similarity metric	Method components optimization	interpolation	Auto	Validation	Data (type)
RIGID						
Yang et al.[269]	Inter-frame phase difference	Least squares	-	Semi	QL, QT	20
Delzescaux et al.[61, 62]	Spatial gradient norm	-	Potential criterion based	Semi	QL, QT	11 (breath-hold)
Bansal et al.[19]	Mutual information	Joint conditional entropy	-	Semi	QL	2
Gupta et al.[92]	Cross-correlation	-	-	Semi	QT	10 (breath-hold followed by free breathing)
Comte et al.[56]	Displacement	Isobarycentric, Least squares	-	Semi	QL, QT	6
Millès et al.[154]	Cross-correlation	-	-	Full	QT	35 (breath-hold)
<i>Intensity based</i>						
Bidaut et al.[30]	Mean squared difference	Least squares	Bicubic	Semi	QL, QT	8
Breeuwer et al.[37, 38]	Normalized cross-correlation	-	Trilinear	Semi	QL	12 (breath-hold)
Bracoud et al.[36]	Mutual information	Gradient descent	Linear	Semi	QL, QT	5
Dornier et al.[68]	Mean squared difference	-	-	Semi	QL, QT	8 (free breathing)
Kawakami et al.[116]	Mean squared difference	M-estimators	Bicubic	Full	QL, QT	4
Sun et al.[231]	Image gradient	-	-	Semi	QL	15
Wong et al.[265]	Normalized mutual information	-	-	Semi	QL, QT	15
Adluru et al.[4]	Normalized mutual information	-	-	Semi	QL, QT	10 (breath-hold)
Kocher et al.[130]	Mean squared difference	Levenberg-Marquardt	-	Semi	QL, QT	10
Schöllhuber et al.[205]	Mutual information	-	-	Full	QL, QT	11
NON-RIGID/ELASTIC						
<i>Feature based</i>						
Gallippi et al.[84]	Intensity based statistical measure	-	-	Full	QL, QT	12 (free breathing)
Gao et al.[86]	-	-	-	Semi	QL	9
Stegmann et al.[226]	Minimum description length	-	-	Full	QL, QT	10 (free breathing)
Ólafsdóttir et al.[171]	Minimum description length, Normalized mutual information	-	-	Full	QL, QT	10 (free breathing)
Tautz et al.[232]	Phase-difference	Variants of gradient-descent and Levenberg-Marquardt	B-splines	Full	QL, QT	8
Wollny et al.[263]	Normalized gradient field / Sum of squared differences	-	-	Full	QL, QT	6 (free breathing)
<i>Intensity based</i>						
Abitir et al.[3]	Localized cross-correlation	Quasi-Newton	B-splines	Semi	QL	8 (breath-hold)
Rougon et al.[189]	Regional correlation & f -information	Gradient-descent	-	Full	QL	15
Li et al.[138]	Custom energy functional	Expectation-minimization	-	Semi	QL, QT	9
Xue et al.[267]	Normalized mutual information	Simple downhill	B-splines	Semi	QL, QT	76
Xue et al.[268]	Localized cross-correlation	-	B-splines	Semi	QL, QT	40

All the registration based methods are enlisted in Table 2.3, along with their constituents discussed earlier. This table also provides a quick overview of the automation extent (semi or full), validation type (qualitative or quantitative), and the number and type (free breathing or breath-hold) of validation datasets.

The rigid and non-rigid registration methods can be further classified into feature and intensity based methods. Feature based methods employ features such as points, surface, landmarks, regions, etc. to maximize the spatial correspondence between the reference and target images. On the other hand, intensity based approaches operate directly on image intensities or their occurrences without prior identification and extraction of features. In most cases, a relation is assumed between intensity values in the sequence and the similarity metric is computed only for the overlapping area between the images being registered.

2.3.1 Rigid transformations based registration methods

Rigid transformations preserve all distances and angles. Methods based on rigid transformations rely on the assumption that motion artifacts lead predominantly to in-plane motion of the object being imaged. The effect of through-plane motion is often not considered due to the sparsity of slices (limited by the image acquisition system). Assuming the non-rigid or elastic deformations of the myocardium in CMRP images to be insignificant, rigid transformation offers a simple yet efficient solution to compensate for translation and rotation of the myocardium over time.

2.3.1.1 Feature based

Rigid transformation based alignment of CMRP images was first employed by Yang et al.[269], who used raw k-space MR data as opposed to the reconstructed data. In their two-step approach, lateral motion correction using the inter frame phase differences of the k-space data was followed by the correction of myocardial boundaries using a cubic B-spline based deformation model; the former step achieved a higher improvement than the latter.

Gradient-based approaches have been applied by several authors. In the approach proposed by Delzescaux et al.[61, 62], the reference image was obtained by computing the maxima of the norm of the spatial gradient of images in a CMRP image sequence. On the reference image thus selected, RV, LV and pericardial contours were traced [61] before the application of an adaptive semi-automatic and self-evaluated registration technique (ASSERT) [61] to reduce in-plane rigid displacements while rejecting the images with non-rigid deformations. These contours were used to build seven registration models and the transformation corresponding to each model was estimated based on potential criterion optimization. For each image, the optimal registration model was selected on the basis of a superimposition score. Following registration, factor images representing myocardial perfusion were obtained by analyzing the registered images with a method called factor analysis for medical image segmentation (FAMIS) [80, 109]. More details on FAMIS are provided in section 2.4.1.1.

Also employing a gradient based strategy, Bansal et al.[19] used an information theoretic registration framework that integrated two channels of information: the pixel intensities and the local gradient information. An ROI defined by myocardial contours on one image was correlated with other images in the sequence. This correlation was

performed by estimating edge probabilities in the target images and modeling with 2D Markov random fields (MRF) [87, 139].

As discussed earlier, an ROI is often used to localize the LV, either manually or automatically. To avoid the tedious manual approach, Gupta et al. [92] localized the LV by utilizing its center of mass and used correlation as the similarity metric. However, as iterations involved in correlation computation may lead to time inefficiency, the images were first converted into binary maps with a threshold-based normalization technique. The constrained search around the center of mass and binary-map thresholding led to a higher robustness in comparison to global search and the subsequent simplification of correlation calculations, respectively.

In contrast to the approach of Gupta et al.[92], the LV was localized manually with an ROI enclosing epi- and endocardial contours in the registration method of Comte et al.[56]. The ROI thus defined was used to generate the reference TICs for the validation. The registration was based on the precise location and tracking of the interface between the left lung and the heart, which served as an anatomical landmark. While the detection of the left lung was performed with region growing and morphological operations, the contour of the heart-lung interface was detected using a Laplacian filter. Each image in the sequence was subsequently aligned to reference image by matching it with reference interface and shifting it on the basis of the displacement calculated using two methods: (i) isobarycentric method, (ii) least squares method; the former was rapid but did not consider rotation. This method was limited by the poor heart-lung interface detection.

Milles et al.[154] incorporated time-intensity variation awareness into their method by applying independent component analysis (ICA) [55, 106] to extract physiologically relevant features together with their time-intensity behavior. The three feature images, one each for the RV, the LV and the baseline, were used to compute a time-varying reference image mimicking intensity changes in the CMRP image sequence. With cross-correlation (CC) as the similarity metric, rigid registration was applied for each slice in a multi-pass and multi-resolution scheme.

2.3.1.2 Intensity based

Bidaut et al.[30] selected one of the images corresponding to the *baseline* of TIC as the reference image, with which the rest of the images in the sequence were matched using pixel-based mean squared differences (MSD) as the similarity metric. In this automatic method, MSD was minimized using a least squares iterative scheme, and a multi-resolution (coarse-to-fine) approach was employed to accelerate the registration process. Until the convergence, the registration process was iterated with an average of all registered images from the last iteration as the new reference image.

Rather than using a reference image, Breeuwer et al. [37, 38] applied the automatic registration on pairs of two successive images in the image sequence considering the information only within an ROI, which was also detected automatically using the method proposed in [225]. The myocardial boundaries were manually drawn on either one arbitrary image or on the maximum intensity projection (MIP) image from the sequence, and were then propagated to the remaining images in the sequence. As an alternative, a completely automatic myocardial boundary detection method [225] was also applied by using constraints on the shape of the myocardium.

In contrast to the methods that include only the LV within the ROI, the rectangular ROIs used by Bracoud et al.[36] and Wong et al.[265] included both the ventricles. While

[36] used a reference image (with constant intensity) in their registration method, [265] applied pair-wise image registration. In both the cases, mutual information (MI) served as the similarity metric; [265] used its normalized form *i.e.*, normalized mutual information (NMI). The rectangular ROI, encompassing both the ventricles [166] was also employed for comparison with a conventional ROI (including only the LV cavity) by Dornier et al.[68]; the latter was called an *optimal mask*. The rigid registration in their method was performed with a continuous model based on B-splines of degree N [236]. Similar to the approach used in [92], position of the LV was assessed by computing its center of mass within the optimal mask. In addition to the residual motion correction of the LV with a registration algorithm, a compartmental model was also used to accurately evaluate the tissue perfusion inside the LV.

A compartmental model was also employed by Adluru et al.[4], but for generating a model image corresponding to each image in the unregistered sequence. The rigid registration was performed twice: first, between the reference image (with optimal contrast between the myocardium and the LV blood pool) and the other images of the sequence within a rectangular mask encompassing only the heart, and later, between the corresponding registered and model images. The model images were obtained after fitting the registered image data (from the first registration) to a two compartment model. For both the instances of registration, MSD was used as the similarity metric.

Gradient-based non-rigid registration strategies have been proposed in [116] and [231]. Kawakami et al.[116] approached the problem of motion correction with a gradient-based image registration method - developed in [164] for automatic alignment of MRI volumes - that allowed a robust estimation of displacement parameters. An M-estimator was used along with the alignment algorithm proposed in [30] to increase the robustness of this estimation [164]. Similarly, Sun et al.[231] introduced an image gradient based similarity metric to reduce the effects of high contrast variation in both cardiac and renal MR perfusion image sequences. Here, the ROI - a bounding box - and the reference image were selected manually before identifying the large translations by tracking the ROI with integer pixel shifts. The rigid registration was assisted by shape priors that were obtained using segmentation with the coupled propagation of epi- and endocardial contours [174].

Shape priors were also used by Schöllhuber et al.[205] in a novel hierarchical pattern matching approach for a robust detection of the heart in CMRP images. The reliance on time-intensity variations was circumvented by locating the heart in distinct time steps. Prior knowledge of the anatomy (diameter and shape of the myocardium) and contrast agent induced intensity variations (minimal gray level variances) were exploited in a hierarchical pattern to locate the best candidate as the ROI with minimal computational costs. The frame at which the heart was detected served as the reference image, and similar to [36] and [265], MI was used as the similarity metric.

A particularly vexing problem in the analysis of CMRP images is the presence of PVE (see section 2.1.3.2), which can lead to unsharp myocardial boundaries - especially epicardial borders- due to dark rim artifacts. To this end, Kocher et al.[130] focused on correcting for PVEs in mixed voxels containing both the myocardial tissue and blood. Similar to several other approaches, the first step in their proposed process involved 2D rigid registration (similarity metric: MI) to remove motion artifacts. From the registered images, the arterial input function (AIF) was estimated by applying a spatial filter within an ROI. This was followed by the investigation of two 1-compartment models for the

reduction of PVE.

2.3.2 Non-rigid/Elastic transformations based registration

Several authors argue that, in addition to in-plane motion induced rigid transformations (translations and rotations), non-uniform cardiac motion and respiration induced through-plane motion may also lead to significant non-rigid/elastic changes (e.g., shape deformation) in the left ventricular geometry [3, 84, 147, 215, 232]. To correct for these deformations, non-rigid transformation based registration techniques are required.

2.3.2.1 Feature based methods

Landmarks were used as features in [84, 226] and [171]. In the method proposed by Gallippi et al.[84], the translations and geometric distortions were corrected using an automatic image registration method that involved the edge-based (3×3 Sobel filter) landmark detection of a few landmarks in the neighborhood of high spatial frequencies. This detection was performed on a template or reference image (center image of the perfusion sequence). Subsequently, each image in the sequence was warped to the template image using a score based on local intensity variation extents, means, variances, and edge directions. For each pixel in the registered perfusion sequence, 7 parameter maps were generated using the corresponding TICs.

Stegmann et al.[226] utilized variance and clustering properties in an annotated training set to develop an unsupervised registration strategy, called cluster aware active appearance model. Here, the time-intensity variations in CMRP images were modeled with a slice-coupled active appearance model (AAM) [57], which was augmented with an minimum description length (MDL) framework [59] for the optimization of landmark correspondences. AAMs provide the advantage of shape and texture based learning along with fast computations, as indicated in the study [171] comparing AAM based approaches to free-form deformation (FFD) based non-rigid registration algorithms. Both the approaches showed similar results in terms of point-to-point errors, but latter performed better when compared on the basis of point-to-curve errors. The advantage of a training procedure was evident from the higher precision values obtained with AAMs in comparison to FFD-based approaches.

Not relying on landmarks, [86] introduced a deformation model based on partial least square regression (PSLR) [260] to extract the intrinsic correlations between the latent factors of both the input (intensity distributions around the chest wall and diaphragm) and the observed output (motion vectors of myocardial deformation). This allowed the extraction of intra-frame tissue deformation, thereby facilitating free-form registration with a dense displacement vector field within the image plane.

Tautz et al.[232] incorporated a multi-scale approach in their non-rigid registration method based on phase-based displacement estimation [77, 129, 149, 150] and the Demons algorithm [237]. To estimate non-rigid deformations, the displacement estimation was implemented in a coarse-to-fine dyadic scale space and the registration was iterated 3 times for successive images in the temporal sequence on each scale to refine the estimation, with the central frame of the sequence serving as the reference image.

As discussed earlier (section 2.1.3.3), CMRP images can also be acquired without a breath-hold constraint. In contrast to a breath-hold CMRP image sequence, a free-breathing sequence exhibits quasi-periodicity [263]. This quasi-periodicity was exploited in [263] for decoupling breathing motion from intensity variation. Their automatic

method involved two steps: (i) identification and registration of a subset of images corresponding to the same phase of the breathing cycle, and (ii) registration of the remaining images to synthetic references, created by linearly combining the registered images from the first step.

2.3.2.2 Intensity based methods

The approach of [3] to non-rigid registration involved a rapid multi-resolution free-form registration method [248] using localized cross-correlation (LCC) as the similarity metric, and the last image in the perfusion sequence as the reference image. Prior to non-rigid registration, the prospective through-plane motion of the LV was corrected with tissue tagging. The remaining in-plane distortion of the heart was removed by recovering the intrinsic relationship between respiration and cardiac deformation using PLSR. Subsequently, perfusion analysis of the registered images was performed with factor analysis by extracting tracer characteristics of different myocardial regions [29, 42, 146].

Rougon et al.[189] proposed a region-driven approach based on regionalized statistical similarity measures: correlation ratio and f - information [244]. A spatial prior was included by means of a reference image associated labeled scene model. The computation of similarity criteria involved regularization [190] and regional probability densities estimation by using specific Parzen kernels defined over each component of the scene. By iteratively adapting the image data to the scene model, joint non-rigid registration and segmentation of the target image were obtained.

Instead of relying on a single reference image, [138] generated a sequence of pseudo ground images and performed non-rigid registration between the corresponding images in the pseudo ground truth and original sequences. The pseudo ground truth estimation and the demons based non-rigid registration [251] were integrated into an energy functional that was iteratively minimized in an expectation-minimization fashion.

The lack of comprehensive validation on large clinical datasets including different CMRP imaging pulse sequences and slice positions motivated Xue et al.[267] to conduct a multi-center study, using a method including both the rigid and non-rigid registration. Multiple levels of resolution and optimization levels were used for rigid registration before the application of a non-rigid registration strategy, involving multi-level B-spline based FFD transformation. With NMI as the similarity metric, registration was performed consecutively between temporally adjacent images, starting from the template (peak intensity image).

A different approach to the reference frame detection, called consecutive motion compensation, was adopted by Xue et al.[268] in the extension of their previous work [267]. Here, the reference frame was detected on the basis of maximum cross correlation ratio between every frame in the perfusion series and the standard deviation (SD) image. The SD image consisted of the regions with highest standard deviation along the time dimension. Subsequently, the reference frame was first non-rigidly registered [48] with its immediate neighbors before multiple non-rigid registrations were performed between temporally adjacent slices. Furthermore, additional steps were included for: (a) surface coil inhomogeneity correction using proton density images, and (b) the generation of a robust parameter map.

Summary

Generally, rigid registration provides more consistent results despite its inability to align the images accurately in case of deformations. Its consistency can be attributed to its ability to align the images using a precise nearest rigid transformation. Although the alignment with nonrigid registration is better, the precision is lower compared to rigid registration. Whereas local deformation values have to be calculated from a subset of image pixels in non-rigid registration, all the pixels in the ROI are employed in rigid registration to calculate the lower dimensional transformation. As a result, rigid registration offers higher robustness to noise and better precision (less than a pixel) than nonrigid registration.

Within rigid and non-rigid registration, feature based strategies achieve faster convergence (due to less iterations of optimization) and sub-pixel accuracies. Nevertheless, they require feature extraction and pre-processing before the actual registration. They are also more susceptible to noise and outliers than the intensity based methods. Compared to feature based methods, intensity based approaches are more flexible, as the information used for the alignment is not restricted to specific features. These methods are often generic, and hence, can be applied to any dataset without pre-processing. In addition, they are robust against noise and insensitive to outliers, as only the intensities are used for registration. However, as the intensity based methods use pixel intensities directly instead of features, they often suffer from difficulties in achieving sub-pixel accuracy and faster convergence.

In addition to the accuracy and robustness, time efficiency of the registration process is a major factor determining its acceptance in the clinics. Several authors have therefore incorporated multi-scale and multi-resolution schemes into their registration approaches. These schemes increase the robustness of registration by initially emphasizing on global, large-scale image structures and then proceeding to further refinement based on small image details.

2.4 Methods based on segmentation

The objective of segmentation is to provide reliable, fast, and effective object recognition and delineation either by clinicians or automatically using robust techniques. Although, segmentation algorithms are often applied on the images that have already been aligned spatially using a registration scheme, some methods use them to aid registration process as well. The segmentation strategies can be classified into model independent and model based approaches (Table 2.3).

2.4.1 Model independent

Model independent segmentation approaches for CMRP image processing often rely on thresholding and clustering based techniques. Techniques based on thresholding assume a relationship between the objects of interest and distinctly quantifiable features such as image intensity and gradient. In clustering methods, the features of the interesting structures are extracted from the already classified points and are updated through iterations.

Spreeuwens et al.[225] proposed a thresholding based method to coarsely segment the LV and RV by searching for the local maxima in space and time. Region growing was applied with the seeds at the RV and LV centers, and their boundaries were extracted by tracing the outlines of the found regions using a polar transformation.

Table 2.5: Segmentation based methods

Authors	Methods (salient features)	Auto	Validation	Data (type)
<i>Model independent segmentation</i>				
Behloul et al.[23]	Fuzzy logic, Fuzzy inference system	Semi	QL	-
Di et al.[63]	Factor analysis, k-means clustering	Semi	QL, QT	2
Spreeuwers et al.[225]	Region growing, Polar transformation, Snakes	Full	QL	14
<i>Model based segmentation</i>				
Boudraa et al.[35]	Parametric modeling	Semi	QT	22 (breath-hold)
Janier et al.[109]	Factor analysis in medical image segmentation	Semi	QL	13
Santarelli et al.[198]	Gradient vector flow snakes, Anisotropic filtering	Full	QL, QT	9
Discher et al.[67]	Bi-ventricular heart template deformation, Level sets	Full	QL, QT	15
Pluempitiwiriyaewj et al.[180]	Stochastic active contour scheme, Thresholding, Median filtering, Morphological operations (closing)	Full	QL	1
Adluru et al.[5]	Level sets	Semi	QL, QT	8
Lorenzo et al.[141]	Shape modeling, Level sets	Semi	QL	16
Baka et al.[17]	Active appearance motion model	Semi	QL, QT	19 (breath-hold)
Gupta et al.[93]	Independent component analysis, Active appearance modeling	Full	QL, QT	18 (breath-hold)

Behloul et al.[23] used clustering based segmentation to perform myocardial boundary detection. A slice from cine-MR images was segmented using fuzzy clustering and fuzzy inference systems (FIS). The segmented cine-MR images were then warped to obtain the desired myocardial boundaries in CMRP images. Here, the ROI was defined manually as a rectangular region on each image of the perfusion sequence. In another clustering based approach [63], automatic grouping and fitting of temporally alike tissue time-signal voxels was performed on the basis of TIC analysis. Two types of TIC analysis techniques, *i.e.*, factor analysis [29] and k-means clustering [235], were explored to extract the blood input function that enabled the automatic fitting of the data to a two-compartment model.

2.4.1.1 Model based

Due to high variability in contrast around the epi- and endocardium, numerous segmentation algorithms use models, such as *parametric* and *deformable* models, that exploit prior knowledge on myocardial shape, texture, size, or location, to identify and delineate the myocardial boundaries.

Several methods used *parametric* models. Boudraa et al.[35] mapped the first-pass transit of contrast bolus through the heart to obtain a similarity map, or parametric image, representing regions with different temporal dynamics. The similarity map was generated by first eliminating the motion artifacts with manual translations, and then estimating the pixel by pixel correspondence to a myocardial reference using a temporal covariance measure. Although the similarity map resembled commonly used bull's eye representation, it offered a better spatial resolution preservation.

Janier et al.[109] used FAMIS [29, 66, 80] to obtain accurate myocardial tissue factor (FAMIS_t) images for the interpretation of perfusion in a selected group of patients with well-documented CAD. FAMIS is based on a statistical model which assumes that a time-varying image sequence can be studied by resolving it into a few spatial distributions, each with homogeneous signal intensity variations. These spatial distributions are estimated by factor images and the functions describing the signal variations are estimated by factors

[29]. Prior to the application of FAMIS, manual translation was applied when necessary on an image-by-image basis, and subsequently, a single FAMIS image was obtained with FAMIS for each raw CMRP image sequence. The efficacy of FAMIS was then evaluated with a multi-case, multi-reader receiver operating characteristic analysis.

Deformable models have been used more often than the *parametric* models. Adluru et al.[5] employed level sets [172] to utilize temporal and spatial information in the perfusion images for the automatic segmentation of the myocardium. Their previous approach [141] was extended here by removing the manual selection of both the myocardial seed points and the shape model. Before the segmentation, CMRP images were rigidly registered to a reference image, which was chosen from the temporal center of the sequence. To perform this registration, spatially weighted MSDs were minimized between the reference frame and other images in the sequence. The segmentation was performed with a level set based framework that incorporated temporal information by using a spectral speed function [46].

Considering the importance of myocardial contour identification and delineation in CMRP image analysis, the popularity of statistical contour based schemes is not surprising. Santarelli et al.[198] applied non-linear and anisotropic smoothing filter to evaluate image gradients, and then the myocardial contours were delineated through a deformable model based on gradient-vector-flow (GVF) snakes [266]. However, this approach required manual tracing of a coarse polygon in the LV for myocardial segmentation. Precluding any manual interaction, model based unsupervised method proposed in [67] involved statistical contour based automatic detection of a bi-ventricular patient-specific heart template on a reference image with maximum myocardial contrast. The template consisted of 4 regions: the thorax, the RV, the LV, and the left myocardium and the curve flow in this segmentation was performed with classical level sets. To ensure the inclusion of only cardiac region, a mathematical morphology [223] based spatio-temporal approach preceded the template detection step. Finally, an intensity based non-rigid registration technique [189] was used to eliminate the motion artifacts. In another contour based approach [180], the problems associated with the presence of papillary muscles around the LV were overcome using the stochastic active contours scheme (STACS) [181].

Information about common variations in the myocardial shape and texture can also be included in the model using statistical shape models, such as AAM. Baka et al.[17] employed multi-banded AAMs [227] with the integration of spatial and temporal characteristics of the perfusion sequence into their segmentation method. Here, the multi-bands comprised different combinations of temporal (related to temporal perfusion profile) and spatial feature images (gradient orientation maps [216]). Four temporal features (calculated pixel-wise) characterizing the TIC, and one spatial feature were examined. The maximum intensity projection feature and gradient orientation map were found to form the best combination, and the addition of more temporal features was deemed redundant.

In another approach utilizing AAMs, Gupta et al.[93] incorporated the prior knowledge on temporal variation in a CMRP sequence by applying ICA to extract physiologically relevant feature images and their corresponding weights, for each time point [154]. In addition to the feature images, initialization parameters and the optimal contrast image were also obtained for the AAM based myocardial segmentation. Based on an ICA based model, a reference image for each time point was computed, with which the corresponding motion affected image was rigidly registered using CC as the similarity metric. The use

of ICA and AAM allowed this approach to be completely independent of any manual interaction.

Summary

As myocardial tissue often has distinctive intensity, choosing threshold-based techniques can be effective and efficient. However, these algorithms are highly sensitive to noise and interference of surrounding structures such as epicardial boundaries. As a result, these algorithms are seldom used alone; instead, they are often used either in combination with other strategies or in segmentation driven registration approaches [19]. Clustering algorithms are computationally efficient, but the number of classes, the position of initial points and other used parameters should be properly determined beforehand in order to get good results.

Model based approaches have been more popular due to their ability to efficiently handle contrast variations in the myocardium. Aided by the inherent a-priori information on shape and structure of the object to be segmented, these approaches are more stable against local image artifacts and perturbations than model-independent algorithms. Among the model based approaches, majority of the methods adopted contour based deformable models, as they can be conformed specifically to myocardial shape and provide good results with appropriate modeling. In addition, they offer sub-pixel accuracy, noise insensitivity, and intuitive interaction mechanisms. However, many model based approaches require either a selection of proper parameters or a training step to achieve desired results. Another limitation of deformable models can be their poor convergence to concave boundaries.

2.5 Methods for multi-modality information fusion and visualization

The myocardium can be studied with different imaging modalities, and each of these modalities provide complementary information about its structural and functional integrity. The first signs of myocardial deterioration are often provided by the analysis of myocardial perfusion, using SPECT, PET or MRI. With MRI, one can look at CMRP or delayed enhancement (DE) images [108, 249] to analyze the extent of deterioration, and to predict the myocardial viability. The later stages of myocardial ischemia can be analyzed using cine-MR imaging, which provides an indication of the contractile function of the ventricular wall [143]. As a result, several methods were proposed to concurrently analyze the information from different modalities either for visualization only, or for more detailed correlation studies. An overview of the combinations from different techniques and modalities is provided in Figure 2.5 and Table 2.6. As discussed earlier, motion correction with rigid or non-rigid registrations is usually the major preprocessing step for the analysis of CMRP images. It is often followed by manual or automatic identification and delineation of the myocardial boundaries. From the region enclosed within these boundaries, the TIC, and subsequently, the perfusion parameters can be obtained. These parameters assist clinicians in detecting as well as locating a defect in the myocardium and assessing its severity, if a defect is present. A bull's eye plot (BEP), based on the American Heart Association's (AHA) 17-segment model [47], is often used to display these parameters. It divides the left ventricle into 17 segments according to the correspondence between the myocardial segments and the supplying coronary branch: ramus circumflex (RCX), left anterior descending (LAD), and right coronary artery (RCA). The 17 segment AHA model

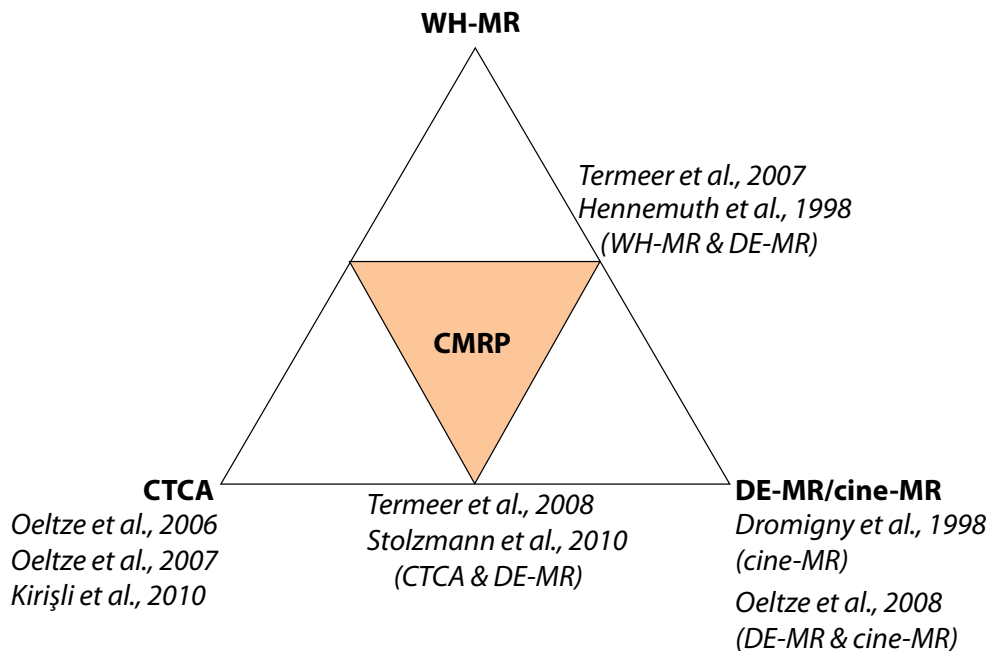


Figure 2.5: Image processing methods for intra- and inter-modality information fusion: The vertices of this triangle represent imaging modalities (or techniques), and an edge connecting any two vertices represents the fusion of the respective modalities.

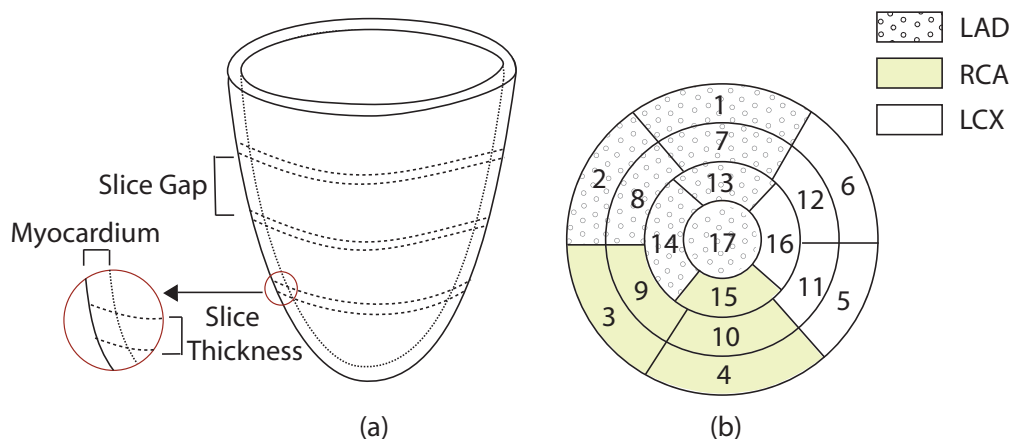


Figure 2.6: The perfusion of (a) left ventricular myocardium is typically shown using (b) a Bull's Eye Plot (BEP) based on American Heart Association's (AHA) 17-segment model.

Table 2.6: Methods for multi-modality information fusion and visualization

Authors	Modalities (in addition to CMRP)	Salient features	Data
Dromigny et al.[69]	cine-MR	Overlay of BEPs	4
Oeltze et al.[168]	CTCA	Combined BEPs	-
Oeltze et al.[169]	CTCA	Combined BEPs, PCA	2
Termeer et al.[233]	DE-MR, WH-MR	VBEP	-
Oeltze et al.[170]	cine-MR, DE-MR	Glyphs	15
Hennemuth et al.[101]	DE-MR, WH-MR	Region growing, Watershed, Live wire	21
Termeer et al.[234]	CTCA, DE-MR	VBEP	-
Kirişli et al.[119]	CTCA	Linkage of 2D BEP & 3D model of the heart	10
Stolzmann et al.[229]	CTCA, DE-MR	Combined BEPs	5

allows the visualization of various perfusion parameters (SI_{peak} , T_{peak} , $Up-slope$, T_{mean} , etc.) through a color-coded BEP as shown in Figure 2.6.

In one of the first applications of information fusion from different MRI techniques [69], cardiac contraction information obtained from cine-MR image sequences was fused with perfusion information from CMRP images. Myocardial boundaries in cine-MR images were detected semi-automatically using the method described in [18]. After the identification of systolic and diastolic images by comparing the region enclosed by endocardial contours, a contraction-map image (two B-spline curves) was obtained to represent the local contraction. Similarly, information from CMRP images was represented in the form of a myocardial perfusion map. The pixel values in this map were proportional to the TIC slope in the same pixel [44]. Due to the complementary information and different representations of contraction and perfusion maps, the two maps could be fused to obtain a new image, in which the contraction and perfusion properties of the myocardium were revealed simultaneously.

Oeltze et al.[168] developed an integrated visualization technique to relate perfusion information from CMRP images to morphological information from CTCA images. From CTCA data, epicardial left ventricle was segmented using live-wire [203] and the coronary tree was extracted using region growing [99] and thinning algorithms [217]. The visualization of the coronaries was implemented using convolution surfaces [167]. Motion correction in the CMRP data was accomplished with a combination of rigid and non-rigid registration algorithms, using MI as the similarity metric [191]. The ROI was defined manually and corresponding TICs were generated to calculate the parameters for each voxel of the dataset. A synchronized visualization allowed exploration of reduced perfusion with the three-dimensional (3D) rendering of the coronary vessels. Multiple perfusion parameters were displayed simultaneously within a single image using the combination of shapes and colors. For instance, a 3D colored height-field display was used to show two different parameters on a single CMRP image; one parameter was represented by the color and the other by the elevation. Colored height fields, in addition to the link with coronary anatomy, further enhanced the voxel-wise analysis of different perfusion parameters. The integration of statistical methods and interactive feature specification in [169] allowed the detection of trends in the data, thus facilitating the detection of suspicious structures and preprocessing failures. Furthermore, dimensionality reduction performed with correlation analysis and PCA [160] provided a better understanding of the inter-parameter relations.

In 2008, Oeltze et al.[170] proposed another visualization framework for the integrated analysis of CMRP, cine-MR and DE-MR data. A glyph based method was employed, and myocardial viability and contractility parameters were displayed in a 3D space. Serving as the reference image, an end-diastolic image from the cine-MR data was used to register: (a) slice-wise DE-MR data using rigid transformations and normalized CC as the similarity metric; and (b) the baseline images (from different slices) in CMRP data using the approach proposed by [100]. For CMRP dataset, the myocardial segmentation was performed in one motion corrected image with Live Wire algorithm [203] before propagating the obtained contours to all the frames of respective slices. In cine-MR images, the segmentation was limited to the end-diastolic and end-systolic phases. A histogram analysis based method [102] was used for the segmentation of scar in DE-MR images. Eventually, glyphs were used to facilitate joint visualization of myocardial perfusion, contractility and viability.

Similar to [170], Termeer et al.[233] also used the data only from MRI but acquired using different techniques. A comprehensive framework for the visualization of coronary artery disease (CoViCAD) was proposed to combine information from 3D Whole Heart-MR (WH-MR) and DE-MR datasets; the former exposed anatomical details and the latter provided scar information. A novel addition to the BEP allowed the linkage of scar to specific coronary arteries. The myocardium was unfolded to extend the existing BEP representation while preserving the volumetric nature of the LV wall. The volumetric BEP (VBEP), thus generated, provided transmural information in association with anatomical information. Additionally, the coronary arteries were also projected on the epicardial surface of the VBEP.

A more advanced mapping between the myocardium and the coronary arteries was established in the extension of CoViCAD framework [234]. A computational simulation was added to indirectly visualize the coronary anatomy, and it was demonstrated that this simulation could provide a more comprehensive visualization of the information in comparison to rendering the anatomical data directly. Coronary blood flow was also modeled by using CTCA images to obtain detailed coronary artery tree segmentation.

Hennemuth et al.[101] proposed an approach for the fusion of myocardial viability and perfusion in an anatomical context. In addition to CMRP image alignment using an approach similar to [170], CMRP and DE-MR images were registered to WH-MR dataset, with WH-MR volume as the reference, and NMI and normalized CC as the similarity metrics. For the coronary tree extraction, a region growing approach was used [34, 99]. The DE-MR images were analyzed with methods based on histogram analysis, constrained watershed segmentation [102] and the Live Wire algorithm [203].

Stolzmann et al.[229] argued that the side by side evaluation of anatomic and functional information from CTCA and CMRP images, respectively, often led to incorrect allocation of vascular territories to myocardial segments [218] due to the mismatch between the standard myocardial distribution territories [47] and actual coronary anatomy [204, 218]. The fusion of images, instead of side by side information visualization, was proposed as a solution. Three characteristic landmark points were defined in CTCA and DE-MR images for rigid registration based alignment. To extract the coronary tree from CTCA images, a region-growing algorithm [32] was used. The extraction of perfusion parameters from CMRP images involved B-spline registration for motion correction and a mixture model for segmentation of the hypoperfused myocardial regions. From the DE-MR images, the extent and location of scar tissue was determined by adopting a

	<i>identification, location, and extent</i>			
Information type	Stenosis / narrowing	Myocardial perfusion defect	Functional abnormality (e.g., wall motion & thickness)	Scar
Imaging modality	CT		MR	
Imaging technique	Coronary Angiography	First-pass perfusion	Cine	Delayed enhancement

Figure 2.7: Common types of information obtained from different cardiac imaging modalities and techniques

strategy similar to [101]. An integrated visualization framework was developed to view registered surfaces and volume renderings of the coronary arteries and LV overlaid with parameters from CMRP (perfusion deficits) or DE-MR (scar tissue).

In the integrated visualization and analysis approach of Kirişli et al. [119], information on coronary artery tree was obtained from CTCA images using a semi-automatic method based on [151, 200], and myocardial perfusion parameters were obtained using QMass MR [148]. To combine information extracted from CTCA and CMRP images, spatial alignment was performed with an iterative closest point approach. The salient features of the proposed visualization were as follows: (a) a 2D projection of the coronary tree on the BEP, (b) the addition of a 3D coronary tree model, and (c) a 3D model of the heart, derived automatically from CTCA images using a multi-atlas based segmentation approach [120]. These components were linked to each other to allow an interactive visualization of the perfusion and coronary anatomy, simultaneously.

Summary

The information fusion approaches in the existing literature focus on combining the information from: (a) different modalities, or (b) different techniques, but common modality (Figure 2.7). An example of multi-parameter visualization is shown in Figure 2.8. A common theme among all these methods is the use of BEP, either in 2D or 3D [234]. Several interactive visualization techniques incorporated both new and established registration and segmentation methods. These techniques employed CTCA images for extracting anatomical details of coronaries, CMRP images to obtain TICs and perfusion parameters, and DE-MR images to identify and locate the scar tissue. In addition, cine-MR images were also used by a few approaches to draw the initial contours for myocardial segmentation in CMRP images. For a detailed description of perfusion visualization approaches, [24] and [182] are recommended.

2.6 Conclusion

We have presented a comprehensive survey of CMRP image processing methods in this article. A broad categorization of all such methods was proposed on the basis of two major image processing components: registration and segmentation. The methods for multi-modality information fusion and visualization were discussed within a distinct category.

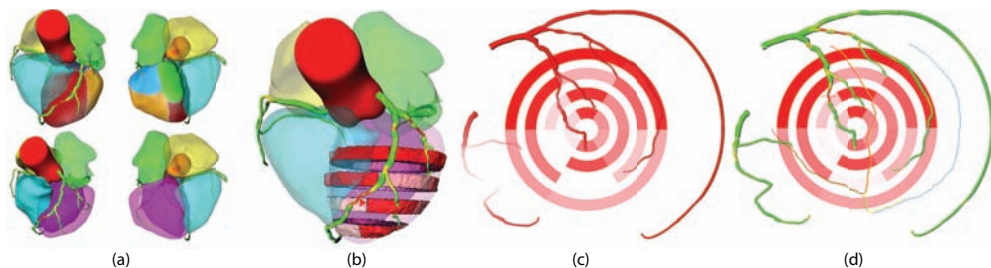


Figure 2.8: An example of multi-parameter visualization: (a) presents a 3D model of the heart, with its coronary artery tree color-coded with the degree of stenosis. On the LV, the patient-specific perfusion territory of the LAD is shown in red, of the LCX in blue, of the Obtuse Marginal branch (MO) in yellow and of the RCA in green. (b) shows how the perfusion information can be integrated into a 3D model of the heart. (c) presents a 2D perfusion bull's eye plot (BEP) with the coronary artery tree projected on top; the more transparent the artery, the further it is from the epicardium. (d) shows a 2D perfusion BEP with both its coronary artery tree and its coronary perfusion territories projected on top; arteries are color coded with the degree of stenosis.

Current approaches and future perspective

CMRP image processing is a complex task due to surface coil related inhomogeneities, image artifacts (PVEs, motion artifacts, etc.), low contrast between the heart and other thorax structures, limited accurate anatomical landmarks, and lower image resolution. Surface coil inhomogeneity is often corrected by using *baseline correction* but proton density images have also been used [268]. PVE correction in image domain has been tried in [130] but it is still limited by image resolution.

Motion artifacts are most prevalent, and are generally eliminated by either rigid or non-rigid registration techniques. While rigid registration corrects for translations and rotations, elastic or non-rigid registration corrects for the deformation of the heart. Although, both rigid and non-rigid registration approaches have shown promising results with respect to accuracy, robustness and automation, there is no consensus regarding the optimal approach. Rigid registration is computationally more efficient, robust to noise, and provides better consistency along with higher precision. However, the rigid alignment does not take into account the through-plane motion and spatial deformation of the heart caused by non-uniform cardiac motion and unintended respiratory motion. Non-rigid registration provides better alignment but with lower precision, and is more susceptible to noise. A promising future avenue in registration of CMRP images would be to consider the motion of the entire heart (e.g., by making a patient specific heart model) taking into account both its non-rigid deformation as well as rigid motion.

Segmentation of the left ventricular myocardium along endo- and epicardial borders is still a very challenging task; in particular, endocardial segmentation is difficult due to trabeculae and papillary muscles, and epicardial segmentation due to image intensity variation in the surrounding structures such as lungs, diaphragm, and epicardial fat. Robust endocardial boundary detection and PVE reduction in CMRP images may be

achieved by a technique similar to the one proposed in [53, 54] for cine-MR images. Here, small trabeculations and papillary muscles were taken into account by assuming that the pixel intensities within the LV endocardial boundary partially contribute to the blood volume and partially to the myocardial mass. For the segmentation of more challenging epicardial contours, deformable model based segmentation approaches, especially the contour based approaches, seem to be more promising. In general, future research in the segmentation of CMRP images is expected to focus more on the deformable model based approaches with further improvements in the complex topology handling capabilities, training and representation of the models.

Multi-modality information fusion and visualization techniques allow visual assessment of the perfusion deficits from CMRP images as well as the display of complementary information from different modalities. At present, these techniques show: (a) different parameters in one image; (b) combined information from the images acquired with different imaging modalities; and (c) several features derived from the image analysis. Several visualization tools have also been used to assist interactive CMRP image analysis: color coding, geometrical shapes (e.g., glyphs), annotations, overlays, magnifiers, and statistical representations (e.g., plots, graphs). While the proposed approaches have been effective in analyzing information from a single patient at a time, true challenges in the future lie in visualizing the information from multiple patients, at multiple time points (e.g., to track the progression of pathology before and after the therapy), and multiple modalities. Furthermore, with the continuous growth in size and complexity of the image data, new techniques will be required to reduce either the dimensionality or the number of data points. This reduction, however, would also necessitate a spatial context to link different representations of the reduced data effectively and across multiple modalities.

Perfusion quantification

Assuming that the motion artifacts are already eliminated by registration techniques and images are segmented manually or automatically using image processing methods, semi- or absolute quantitative perfusion analysis can be performed. The quantification of perfusion allows the measurement of absolute myocardial blood flow. However, the accuracy of this measurement is limited by the inability of perfusion quantification approaches to measure the arterial input accurately and relatively closer to the myocardial region of interest. Considering the rapid innovations in perfusion quantification field, the standardization is difficult and consensus on optimal approaches may therefore take more time.

Clinical acceptance of CMRP imaging processing methods

Considerable success has been achieved by the reviewed methods with respect to the technical developments and extent of automation. Although several artifacts influencing the quantitative analysis in CMRP images have been overcome with the use of these methods, their acceptance in clinical routine is still limited. Two major drawbacks seem to be responsible for this limited acceptance. First, it involves a steep learning curve for the clinicians to use these methods without their integration into user friendly frameworks. Second, their acceptance is significantly hampered by the absence of algorithmic validation with multi-vendor and multi-center datasets. To address these issues, it is, therefore, essential to (a) integrate the robust post-processing techniques into user-friendly software packages (e.g., [98, 148]), and (b) create a publicly available database of a few multi-

vendor and multi-center datasets so that an unbiased evaluation of these methods could be performed in a systemic way similar to the MICCAI challenges [152]. As it stands now, it is difficult to comment on the clinical acceptance of surveyed methods due to the scarcity of published data on the integration of these methods in commercial softwares.

In conclusion, the challenges posed by the rapid developments in CMRP imaging are often difficult to meet with the advancements in image acquisition systems and protocols alone. For the CMRP imaging to become a routinely used modality in the non-invasive assessment of CAD, it is therefore essential that it is augmented with image processing methods, which must continue to evolve, both with respect to functionality, and with respect to evaluation.

Appendix A

Several aspects of CMRP image acquisition, perfusion quantification, image artifacts and general image processing methods, which could not be discussed in the main body of this chapter, have been discussed at length in few of the latest review/survey articles that are enlisted in Table 2.7.

Table 2.7: Review and survey articles for further reading

Authors (year)	Topic
Mäkelä et al.[142]	Cardiac image registration methods
Kellman et al.[118]	CMRP imaging sequences
Gerber et al.[88]	CMRP imaging: history and state of the art
Scott et al.[215]	Motion in cardiovascular imaging
Attili et al.[14]	Quantification in cardiac MRI
Beller et al.[27]	Multimodality cardiac imaging
Jerosch-Herold et al.[110]	Quantification of myocardial perfusion with MRI
Preim et al.[182]	Visual exploration & analysis of perfusion data
Beller et al.[27]	Current & future trends in multi-modality cardiac imaging
Sourbron et al.[224]	Technical aspects of MR perfusion

